Rapid Transitions in Zonal Wind Around the Tropical Tropopause and their Relation to the Amplified Equatorial Kelvin Waves

Noriyuki Nishi[1], Junko Suzuki[2], Atsushi Hamada[1], and Masato Shiotani[2]
[1]*Division of Earth and Planetary Sciences, Graduate School of Science, Kyoto University, Kyoto, Japan*
[2]*Research Institute for Sustainable Humanosphere, Kyoto University, Kyoto, Japan*

Abstract

Rapid transitions in the zonal wind (U) around the tropical tropopause within several days are investigated by using the global analysis data and their relation to the amplified Kelvin waves are considered. At 100 hPa, cases with a rapid increase in U (TypeU+ events) are concentrated in the eastern hemisphere, where such cases far outnumber cases that show a rapid decrease in U (TypeU− events). The difference in the number of the two types of events is greatest during the period November–March in the region 90°E–180°E. When only considering cases with a large zonal extent and eastward propagation, the dominance of TypeU+ events in the eastern hemisphere is much more distinct. The asymmetry between the two types is only weakly recorded at lower levels. An amplified and nonlinearly distorted Kelvin wave possibly accounts for predominance of these TypeU+ events at 100hPa. The dominance of TypeU+ events is detected in the basic easterly flow within the upper troposphere, which possibly facilitates the distortion by enhancing the upward propagation of energy and enabling the high intrinsic speed of the wave. In the distorted Kelvin wave, the latitudinal extent of the westerly signal is much smaller than that of the easterly signal.

1. Introduction

On the basis of radiosonde observations, Tsuda et al. (1994) reported the existence of an equatorial-trapped Kelvin wave (hereafter simply referred to as the "Kelvin wave") with an extremely large amplitude and confined to the tropopause region. Shimizu and Tsuda (1997) undertook a statistical study of the Kelvin wave using a longer record of radiosonde observation. Recently, Suzuki and Shiotani (2005) used global analysis data to conduct a statistical analysis of the Kelvin wave near the tropopause level to determine the statistical distribution of the seasonal and longitudinal variability of the wave. These studies revealed that the wave has a longer period and smaller phase speed than the well-known stratospheric Kelvin wave first reported by Wallace and Kousky (1968).

Nishi and Sumi (1995) undertook a case study of the Kelvin wave during January–February 1993 using Japan Meteorological Agency global analysis data. The authors found that the region with large amplitudes does not extend around the entire equator: it is limited to several ten-degree longitudes, and the wave shows a significant distortion from a sinusoidal wave form within this region. The distortion is represented by a rapid shift from an easterly to westerly phase. The basic idea of the distortion mechanism is rather simple: the distortion is considered to result from a nonlinear effect in the finite amplitude wave, and it can be described using the one-dimensional advection equation (e.g., Boyd 1980).

A study of waves in the tropopause region is of interest in the field of wave dynamics because the region is in the near-field of the main source of the wave in the troposphere and has complicated basic fields such as large horizontal and vertical wind shear and a large vertical gradient of static stability. As the large wind shear or breaking that can occur following distortion of the wave can lead to large-scale mixing (Fujiwara et al. 1998, 2003; Fujiwara and Takahashi 2001), the present study is also important in terms of transport problems in the tropical tropopause region.

As Nishi and Sumi (1995) only analyzed data over a 2-month period, the present study attempts to elucidate the statistical seasonal and longitudinal distribution of the occurrence of the distortion, and we introduce some interesting features in terms of the distortion shape of the wave as determined from a 23-year dataset.

2. Data and analysis methods

We use the ERA-40 global reanalysis dataset produced by the European Centre for Medium-range Weather Forecasts (ECMWF) with a 2.5° grid and 6-hourly resolution for the period 1979–2001. After calculating daily mean values, we attempted to identify rapid transitions in U within 5 days to detect distortion of the Kelvin wave, since the rapid transition associated with the distorted Kelvin wave has a time scale of several days (see Nishi and Sumi 1995). We obtained the rate of change ΔU (m s^{-1} day^{-1}) by calculating a linear regression for U over 5 consecutive days at each grid point just on the equator. Note that the selection of suitable cases was performed on simple daily mean series without any filtering on specific waves such as the Kelvin wave. We treat cases with a maximum of $|\Delta U|$ greater than 8 m s^{-1} day^{-1} as cases of rapid transition.

We utilized a filter in wavenumber-frequency space (designed by Wheeler and Kiladis 1999) with a set of cut-off parameters adequate for U at 100 hPa to identify Kelvin wave signal: only the eastward-moving component with 1–12 wavenumbers, periods of 2.5–30 days, and equivalent depths are 8–240 m for the Kelvin wave.

3. Results

3.1 Examples

Figure 1 shows a longitude-time section of two typical cases of rapid transition along the equator at 100 hPa. The color scale in Fig. 1 shows ΔU as defined in Section 2. Figure 1a shows a case in late March 1987 with a remarkably large zonal extent. An easterly flow of greater than 10 m s^{-1} is located around 0°E–60°E on 12 March and moves to the region around 160°E on 25

Corresponding author: Noriyuki Nishi, Division of Earth and Planetary Science, Graduate School of Science, Kyoto University, Kitashirakawa Oiwake, Sakyo, Kyoto 606-8502, Japan. E-mail: nishi@kugi.kyoto-u.ac.jp.

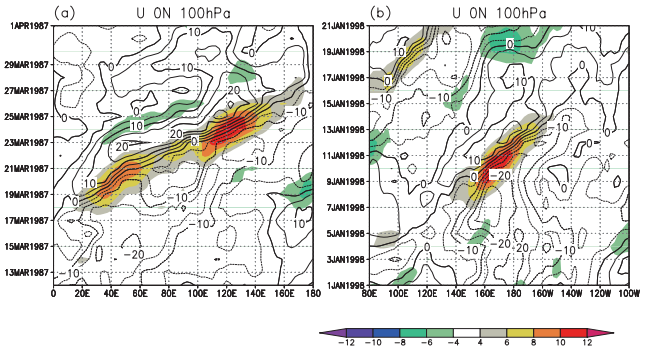

Fig. 1. Examples of Kelvin waves distorted from a sinusoidal form: longitude-time section along the equator (0°N) at 100 hPa. Contours show the zonal wind (m s^{-1}); the contour interval is 5 m s^{-1} and the easterly flow is shown by dashed lines. The color scale shows ΔU (m s^{-1} day^{-1}); see the text for the definition of ΔU. (a) Case for March 1987, and (b) case for January 1998.

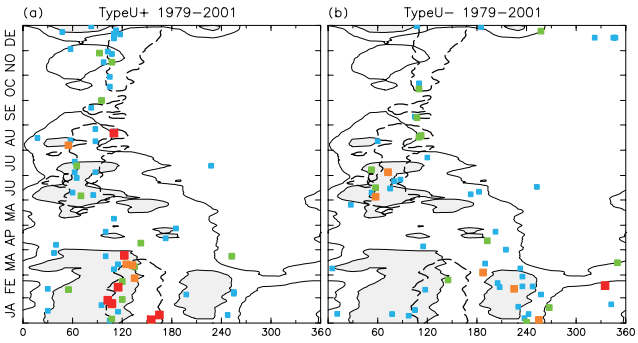

Fig. 2. Longitude-time distribution of cases with a rapid transition in U along the equator at 100 hPa during the period 1979–2001. (a) Cases with a rapid increase in U (TypeU+ events) and (b) those with a rapid decrease in U (TypeU– events). Blue squares represent cases with |ΔU| in excess of 8 m s^{-1} day^{-1}; green squares indicate more than 9 m s^{-1} day^{-1}; orange indicate more than 10 m s^{-1} day^{-1}; and red indicate more than 11 m s^{-1} day^{-1}. Solid lines represent Kelvin wave variance of 11 and 14 m^2 s^{-2}, and the shaded region represents variance of greater than 14 m^2 s^{-2}. The area surrounded by the thick dashed line indicates the strong easterly flow (< −10 m s^{-1}) in the climatological U at the level.

March. The following westerly flow stronger than 10 m s^{-1} is located around 40°E on 21 March and moves to 140°E on 26 March. Between the two wind regions, a region of large positive ΔU is located at 30°E–140°E with interruption near its center. Figure 1b shows a case in late January 1998 with typical extent and speed. A rapid increase in U is detected between 155°E and 175°W during 8–12 January, and the region moves eastward. Two other cases observed during January 1993 are described in Nishi and Sumi (1995). These rapid increases in U associated with the Kelvin wave are interpreted in the present analysis as a "distorted Kelvin wave."

3.2 Longitude-season distribution of TypeU+ and TypeU– events

From the theory of nonlinear wave dynamics, the distortion of a Kelvin wave is expected to have a form with a rapid transition from *easterly* phase to *westerly* phase (e.g., Boyd 1980). First, we examine whether rapid increases in U (TypeU+ event) occur more frequently than rapid decreases in U (TypeU– event) (Fig. 2). We count the number of independent TypeU+ events by selecting all the longitudinal grid points at each day that have maximum value in a box of 200°-longitude and a 21-day extent centered on them. In a similar way, we count the number of negative maxima for TypeU– events. Analysis of the 23-year record reveals 67 TypeU+ and 55 TypeU– events. Comparison of the two panels in Fig. 2 reveals that the number of TypeU+ events in the eastern hemisphere is greater than the number of TypeU– events. In detail, the dominance of TypeU+ events is well detected during November–March, while similar numbers of the two types are recorded during June–August. The most striking feature in the figure is the concentration of TypeU+ events during January–March in the region 90°E–180°E; the ratio of TypeU+ events to all events is 0.83. The asymmetry between the number of both types is even more remarkable for extremely large-magnitude events (|ΔU| > 10 m s^{-1} day^{-1}); all of these cases are TypeU+ events. In contrast, during the northern winter over the western hemisphere, the number of TypeU– events exceeds the number of TypeU+ events.

We examined the relation between the observed rapid transitions and Kelvin wave activity. Figure 2 also shows the variance of the filtered Kelvin wave averaged over the 23-year study period; this was first shown by Suzuki and Shiotani (2005). In the figure, the distribution of both TypeU+ and TypeU– events is largely within the region of large Kelvin wave variance. This implies that a high degree of Kelvin wave activity plays an important role in the occurrence of rapid transitions. The variance of the Kelvin wave shows a close relation to the basic easterly flow (shown by a dashed line in Fig. 2); the relations among the basic zonal wind, Kelvin wave activity, and the rapid transition events will be discussed in Section 4.

3.3 Differences in the shapes of TypeU+ and TypeU– events

In the course of inspecting the different cases, we noticed that a greater number of TypeU+ events than TypeU– events showed a large zonal extent and eastward propagation of the rapid transition region, as illustrated in the examples shown in Fig. 1. Next, we describe differences in the shapes of TypeU+ and TypeU– events.

For each case plotted in Fig. 2, we examined the longitudinal extent and the propagation direction of the rapid transition region. We define the longitudinal range with |ΔU| greater than 7 m s^{-1} day^{-1} as extent of the rapid transition region. To examine the propagation direction, date with maximum |ΔU| is picked out at each longitudinal point. For the longitudinal points with |ΔU| in excess of 5 m s^{-1} day^{-1}, the dates are linearly regressed on the longitude. These operations are applied to the data within a box (75° longitude × 9 day) centered on the point with maximum |ΔU| in each case.

We selected cases from all TypeU+ and TypeU– events on the basis of the following criteria (the selected events are shown in Fig. 3): (1) no westward propagation and (2) extent greater than 20° or 30°. The asymmetry in the number of TypeU+ events (23 cases) and TypeU– events (10 cases) shown in Fig. 3 is much more pronounced than that in Fig. 2. Furthermore, when limited to the eastern hemisphere, the number of TypeU+ events (21 cases) is five times greater than that of TypeU– event (4 cases). TypeU– events has only a small number in the figure, and they show no distinct temporal or spatial concentration.

We undertook a further analysis to confirm that a principal entity of the observed rapid transition is Kelvin wave, rather than MJO with similar eastward-moving property but rather longer period and slower

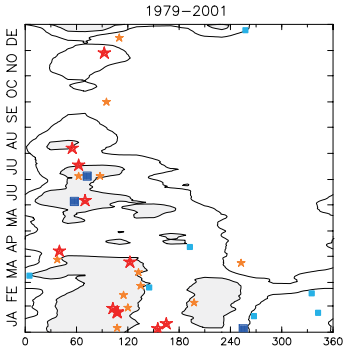

Fig. 3. Longitude-time distribution of cases with large zonal extent and eastward movement of the rapid transition region. Orange and red stars indicate TypeU+ events with zonal extent greater than 20° and 30°, respectively. Light blue and dark blue squares represent TypeU− events with zonal extent greater than 20° and 30°, respectively. See text for details of the criteria used in the selection of events. Solid lines indicate Kelvin wave variance of 11 and 14 $m^2 s^{-2}$, and the shaded region represents variance of greater than 14 $m^2 s^{-2}$.

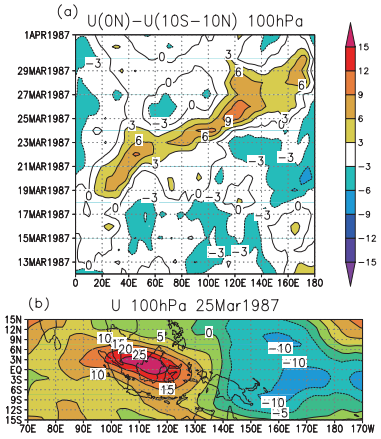

Fig. 4. (a) Longitude-time section of the difference between U along the equator and averaged U within 10°S-10°N (m s^{-1}) at 100 hPa for the case of late March 1987. Contour interval is 3 m s^{-1}. (b) Map of U at 100 hPa on 25 March 1987. Contour interval is 5 m s^{-1}.

phase speed by comparing ΔU with the change rate of the time series filtered to the Kelvin wave mode (ΔU_{KEL}) on the day of the maximum value of |ΔU| in each case. Surprisingly, all the centers of all 67 TypeU+ events show positive ΔU_{KEL} values. This finding demonstrates the close association between the Kelvin wave and TypeU+ events; if the Kelvin wave was not related to the rapid transition, we would expect the rate of positive ΔU_{KEL} to be only about 50%. We also calculated the transition rate of the time series filtered to MJO (ΔU_{MJO}: only the eastward-propagating component with wavenumbers 1–12 and periods of 30–96 days). Approximately 78% of TypeU+ events showed positive ΔU_{MJO} values in their central areas. The rate is much lower than the rate calculated for the Kelvin wave (100 %). Furthermore, our analysis reveals that the speed of the eastward propagation of the rapid increase in U is more similar to that of the Kelvin wave than MJO (not shown). While some TypeU+ events may result from MJO and/or superposition of the Kelvin wave and MJO to bring about a greater magnitude of ΔU, the association with the Kelvin mode is much stronger than that with MJO.

3.4 Latitudinal structure of the distorted Kelvin wave

One interesting feature of TypeU+ events with the Kelvin wave is the latitudinal structure (Fig. 4). The region with positive U value is more strictly confined to the equator than that with negative one. Figure 4a shows a longitude-time section of the difference between U on the equator and the average U within the zone 10°S-10°N for late March 1987. The peaks of the positive and negative value of plotted differences in Fig. 4a lie in the westerly and easterly regions in Fig. 1a, respectively. The magnitude of the difference is much greater in the westerly region of the wave (most pronounced at 120°E on 25 March) than in the easterly region that appeared earlier. A snapshot of the day with the maximum difference is shown in Fig. 4b. The meridional extent of the easterly region around 150°E–180°E is much larger than that of the westerly region around 90°E–130°E. A similar asymmetry in latitudinal extent is also confirmed for most of the TypeU+ events with remarkable large ΔU (greater than 10 m s^{-1} day^{-1}), including the January 1998 case introduced in Fig. 1b (not shown) and the January 1993 cases (a brief comment on this feature can be found in the description

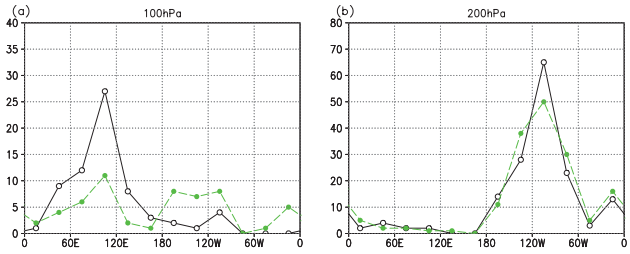

Fig. 5. Longitudinal distribution of the total number of cases with rapid transition (a) at 100 hPa, and (b) at 200 hPa. The black solid line shows the number of TypeU+ events, and the green dashed line shows the number of TypeU− events.

of Fig. 7 in Nishi and Sumi 1995). While we consider that this asymmetry in the latitudinal extent is probably induced by a nonlinear process or presence of another wave superposed in a part of Kelvin wave, the details of the mechanism are the subject of a future study. It should be noted that meridional averaging around the equator may not be adequate for the analysis of the distortion of Kelvin waves.

3.5 Vertical distribution of the rapid transition

Finally, we demonstrate that the asymmetry in the numbers of TypeU+ and TypeU− events is confined to around the tropopause. Figure 5 shows the frequency of rapid transitions in U within each 30° longitudinal zone.

At 100 hPa (Fig. 5a), the number of TypeU+ is greatest in the zone 90°E–120°E for both types (See also Fig. 2). The number of TypeU+ events in this zone is more than twice that of TypeU− events. In contrast, the number of TypeU+ events is so small and less than that of TypeU− events in the western hemisphere.

The longitudinal distribution at lower levels is considerably different from that at 100 hPa. At 200 hPa (Fig. 5b), an extremely large number of events are recorded in the western hemisphere; the peak within 120°W–90°W is more than twice the maximum number at 100 hPa within 90°E–120°E. In contrast, the number of events in the eastern hemisphere, where so many TypeU+ events are detected at 100 hPa, is much smaller than that at 100 hPa. One interesting point in observations at 200 hPa is that unlike the data for 100 hPa, the numbers of TypeU+ and TypeU− events are similar

throughout all zones. At 150 hPa (not shown), the distribution comprises a mixture of the features observed at 100 and 200 hPa; the number of TypeU+ events is greater than that of TypeU− events in the eastern hemisphere, as with the data for 100 hPa, but the number of events has a maximum in the western hemisphere, as with the data for 200 hPa. At 70 hPa (not shown), a predominance of TypeU+ events is also detected, although only a small number of events were recorded.

The differences among different levels may be interpreted to reflect the distance from the wave source: the level of 200 hPa is too close to the wave source to establish the distortion. Another possibility is that the level at 200 hPa is still within the exciting region of the wave; consequently, free-wave dynamics do not apply at this level. In contrast, at the level of 100 hPa, which is about 4 km above 200 hPa, the wave has experienced sufficient time out of the excitation region to become amplified and distorted by the effect of decreasing density and other factors.

4. Summary and discussion

We use a 23-year record of ERA-40 data to analyze the rapid transition of U (within several days) around the tropical tropopause. At 100 hPa, cases with a rapid increase in U (TypeU+ events) are concentrated in the eastern hemisphere, and in this region the TypeU+ events far outnumber those events with a rapid decrease in U (TypeU− events). The difference in the number of cases of each type is greatest within 90°E–180°E during November–March. When limited to cases with large zonal extent and eastward propagation, the dominance of TypeU+ events in the eastern hemisphere is even more pronounced. The asymmetry in the number of cases of each type is not well detected at lower levels. An amplified and nonlinearly distorted Kelvin wave possibly accounts for predominance of TypeU+ events at 100hPa.

Easterly basic wind probably brings the frequent appearance of TypeU+ events in the eastern hemisphere by the following two mechanisms leading to amplification and resulting distortion of Kelvin wave. The first is sufficient amplification of the wave. In Suzuki and Shiotani (2007), the ratio of the variance of filtered Kelvin mode at 100 hPa to that at 150 hPa is 1.5–2 around 90°E and 0.5–0.9 around 240°E with small seasonal variation; the degree of amplification is very different in both hemisphere. The coincidence of the region and season between the large variance of Kelvin wave and the basic easterly flow (Fig. 2) may be explained with the effect of basic wind on the upward wave propagation (Suzuki and Shiotani 2007). While the westerly flow prevents the Kelvin wave from propagating upward, the easterly flow enables the propagation, as explained on the vertical propagation of gravity waves by Kawatani et al. (2005). The second condition is high intrinsic wave speed (C_{INT}). Kelvin wave at 100 hPa has rather fixed phase speed for ground of 10–30 m s^{-1} (Suzuki and Shiotani 2005), probably because the speed of wave source for ground in the lower levels, where basic wind is rather weak, has little longitudinal and seasonal variability (Wheeler and Kiladis 1999). Strong basic easterly flow in the upper troposphere leads to the large magnitude of C_{INT} at the level. Large value of C_{INT} enables a distortion with large amplitude before breaking that occurs when wave amplitude almost equals to C_{INT}.

Two questions remain in terms of the distribution of distortion cases at 100 hPa. 1) During the northern summer, the numbers of TypeU+ and TypeU− events in the eastern hemisphere are similar, unlike other seasons, even though the basic wind is the easterly flow and the variance of the Kelvin wave is relatively large in that season. This leads to the question of why the predominance of TypeU+ events is particularly well observed outside of the northern summer. 2) The frequency of rapid change in the western hemisphere is distinctly biased toward TypeU− events (Fig. 5a). TypeU− events show many cases with lesser eastward propagation and smaller extent (Fig. 3). Therefore, it is important to determine the kinds of disturbances/waves that bring about the dominance of TypeU− events with relatively small extent in the western hemisphere. Since the eastern Pacific region is in the westerly duct, Rossby wave intruding from mid-latitude may have some contribution. An approach based on ray tracing theory should be undertaken to solve these problems.

Acknowledgments

The authors thank Dr. H. Mukougawa, Dr. T. Satomura, Dr. M. Yamada, Dr. T. Nasuno, and Dr. T. Horinouchi for helpful discussions. Analyses and figures were created using the GFD-Dennou Library and the Grid Analysis and Display System (GrADS).

References

Boyd, J. P., 1980: The nonlinear equatorial Kelvin wave. *J. Phys. Oceanogr.*, **10**, 1–11.

Fujiwara, M., K. Kita, and T. Ogawa, 1998: Stratosphere-troposphere exchange of ozone associated with the equatorial Kelvin wave as observed with ozonesondes and rawinsondes. *J. Geophys. Res.*, **103**, 19173–19182.

Fujiwara, M., and M. Takahashi, 2001: Role of the equatorial Kelvin wave in stratosphere-troposphere exchange in a general circulation model. *J. Geophys. Res.*, **106**, 22763–22780.

Fujiwara, M., M. K. Yamamoto, H. Hashiguchi, T. Horinouchi, and S. Fukao, 2003: Turbulence at the tropopause due to breaking Kelvin waves observed by the Equatorial Atmospheric Radar. *Geophys. Res. Lett.*, **30**, doi:10.1029/2002GL016278.

Kawatani, Y., K. Tsuji, and M. Takahashi, 2005: Zonally non-uniform distribution of equatorial gravity waves in an atmospheric general circulation model. *Geophys. Res. Lett.*, **32**, L23815, doi:10.1029/2005GL024068.

Nishi, N., and A. Sumi, 1995: Eastward-moving disturbance near the tropopause along the equator during the TOGA COARE IOP. *J. Meteor. Soc. Japan*, **73**, 321–337.

Shimizu, A., and T. Tsuda, 1997: Characteristics of Kelvin waves and gravity waves observed with radiosondes over Indonesia. *J. Geophys. Res.*, **102**, 26159–26171.

Suzuki, J., and M. Shiotani, 2005: Space-time variations of equatorial Kelvin wave activity and intraseasonal oscillation around the tropical tropopause region. *The proceeding of the third KAGI21 international symposium.* (in press).

Suzuki, J., and M. Shiotani, 2007: Space-time variations of equatorial Kelvin wave and intraseasonal oscillation around the tropical tropopause region. (Available from http://www.rish.kyoto-u.ac.jp/labs/shiotani_lab/members/suzu/paper/ss2007.pdf)

Tsuda, T., Y. Murayama, H. Wiryosumarto, S.-W. B. Harijono, and S. Kato, 1994: Radiosonde observations of equatorial atmosphere dynamics over Indonesia. 1. Equatorial Waves and diurnal tides. *J. Geophys. Res.*, **99**, 10491–10505.

Wallace, J. M., and W. E. Kousky, 1968: Observational evidence of Kelvin waves in the tropical stratosphere. *J. Atmos. Sci.*, **25**, 900–907.

Wheeler, M., and G. N. Kiladis, 1999: Convectively coupled equatorial waves: Analysis of clouds and temperature in the wavenumber-frequency domain. *J. Atmos. Sci.*, **56**, 374–399.

Manuscript received 13 November 2006, accepted 27 December 2006
SOLA: http://www.jstage.jst.go.jp/browse/sola/